^{99m}Tc-interleukin-2 scintigraphy for the in vivo imaging of vulnerable atherosclerotic plaques

Alessio Annovazzi[1], Elena Bonanno[2], Marcello Arca[3], Calogero D'Alessandria[1], Antonella Marcoccia[4], Luigi G. Spagnoli[2], Francesco Violi[4], Francesco Scopinaro[1], Giorgio De Toma[5], Alberto Signore[1, 6, 7]

[1] Nuclear Medicine, 2nd Faculty of Medicine, University La Sapienza, Rome, Italy
[2] Department of Biopathology and Diagnostic Imaging, University Tor Vergata, Rome, Italy
[3] Department of Clinical and Applied Medical Therapy, 1st Faculty of Medicine, University La Sapienza, Rome, Italy
[4] Medical Clinical Institute 1, 1st Faculty of Medicine, University La Sapienza, Rome, Italy
[5] Department of Surgery Pietro Valdoni, 1st Faculty of Medicine, University La Sapienza, Rome, Italy
[6] Department of Nuclear Medicine, University of Groningen, Groningen, The Netherlands
[7] Nuclear Medicine, Ospedale S. Andrea, Via di Grottarossa 1035, 00189 Roma, Italy

Received: 4 May 2005 / Accepted: 4 July 2005 / Published online: 12 October 2005

Abstract. *Purpose:* Several histopathological studies have demonstrated that vulnerable plaques are enriched in inflammatory cells. The aims of this study were: (1a) to test the ability of ^{99m}Tc-labelled interleukin-2 (^{99m}Tc-IL2) to bind to IL2R-positive (IL2R+) cells in carotid plaques and (1b) to correlate the plaque uptake of ^{99m}Tc-IL2, measured in vivo, with the number of IL2R+ cells within the plaque, measured ex vivo by histology (transversal study, TS), and (2) to evaluate changes in ^{99m}Tc-IL2 uptake in plaques, before and after treatment with a statin or a hypocholesterolaemic diet (longitudinal study, LS).
Methods: Ultrasound scan was performed for plaque characterisation and localisation. Fourteen patients (16 plaques) eligible for endoarterectomy were recruited for the TS and underwent ^{99m}Tc-IL2 scintigraphy before surgery. Nine patients (13 plaques) were recruited for the LS; these patients received atorvastatin or a standard hypocholesterolaemic diet and ^{99m}Tc-IL2 scintigraphy was performed before and after 3 months of treatment.
Results: The degree of ^{99m}Tc-IL2 uptake was expressed as the plaque/background (T/B) ratio. In patients from TS, T/B ratios correlated with the percentage of IL2R+ cells at histology (r=0.707; p=0.002) and the number of IL2R+ cells at flow cytometry (r=0.711; p=0.006). No correlations were observed between ultrasound scores and either scintigraphic or histological findings. In patients from the LS, the mean ^{99m}Tc-IL2 uptake decreased in statin-treated patients (1.75±0.50 vs 2.16±0.44; p=0.012), while it was unchanged in the patients on the hypocholesterolaemic diet (2.33±0.45 vs 2.34±0.5).
Conclusion: ^{99m}Tc-IL2 accumulates in vulnerable carotid plaques; this accumulation is correlated with the amount of IL2R+ cells and is influenced by lipid-lowering treatment with a statin.

Keywords: Carotid arteries – Inflammation – Interleukin-2 – Plaque

Eur J Nucl Med Mol Imaging (2006) 33:117–126
DOI 10.1007/s00259-005-1899-4

Alberto Signore (✉)
Nuclear Medicine,
Ospedale S. Andrea,
Via di Grottarossa 1035,
00189 Roma, Italy
e-mail: alberto.signore@uniroma1.it
Tel.: +39-06-33274525
Fax: +39-06-33274521

Introduction

Recent studies have definitively demonstrated that atherosclerosis is to be considered an inflammatory disease [1]. Moreover, there is evidence that the activation of the inflammatory process within the plaques plays a crucial role in promoting plaque rupture and clinical events [2, 3]. Atherosclerotic plaques causing clinical events are often called "vulnerable" or "unstable" [4], and histopathological studies have demonstrated that in these plaques at least 20% of infiltrating cells are lymphocytes, most of which are activated [3, 5, 6]. Activated T lymphocytes can stimulate macrophages to produce metalloproteases, causing plaque instability [7]. Against this background, non-invasive in vivo detection of activated lymphocytes and monocytes in atherosclerotic plaques could provide useful information permitting identification of plaques prone to rupture or complications.

Many radiological techniques are currently used for the diagnosis of atherosclerotic plaques, including angioscopy, angiography, intravascular ultrasonography, echo-Doppler, computed tomography (CT) scan and magnetic resonance

imaging (MRI). All these techniques, however, can only evaluate morphological alterations of vessels, such as reduction of the lumen or thickening of the vessel wall. Nevertheless, MRI is able to provide information on plaque composition, but not on the nature and presence of infiltrating cells [8].

As far as nuclear medicine techniques are concerned, many tracers have been proposed for the study of atherosclerotic plaques, including ^{99m}Tc-labelled low-density lipoproteins [9–12], ^{18}F-fluorodeoxyglucose (^{18}F-FDG) positron emission tomography (PET) [13–18], ^{99m}Tc-annexin-V [19], ^{111}In-human polyclonal immunoglobulins [20], ^{99m}Tc-antisense oligonucleotides [21] and others [22].

IL2 is a cytokine that acts by binding to its receptor (IL2R), expressed mainly on activated T lymphocytes [23]. Scintigraphy with ^{123}I- or ^{99m}Tc-labelled IL2 has been used to image chronic inflammatory disorders [24, 25].

The main aim of the present study was to evaluate whether ^{99m}Tc-IL2 is taken up by carotid plaques in vivo and whether the degree of uptake correlates with either histological/cytological or ultrasound plaque features. Furthermore, in an interventional study, we evaluated whether the degree of ^{99m}Tc-IL2 uptake was influenced by lipid-lowering therapy with a statin or a hypocholesterolaemic diet.

Materials and methods

Patients

Two groups of patients were enrolled in this study. Group A (transversal study) comprised 14 patients (16 plaques) (ten males and four females; age 74.6±8.7 years) with carotid atherosclerosis who showed a stenosis of more than 80% and were candidates for endoarterectomy (the inclusion criteria). Table 1 summarises the main clinical features of these patients. Group B (longitudinal study) comprised 11 patients with carotid atherosclerosis who had a stenosis of less than 80% and who presented an ultrasound pattern of "vulnerable" plaques (the inclusion criteria). Six were randomly assigned to atorvastatin, a synthetic lipid-lowering agent acting via hydroxymethylglutaryl Co-A (HMG-CoA) reductase inhibition, and five, to a hypocholesterolaemic diet. Two patients on the diet exited the study during the follow-up because they refused to maintain the diet. Therefore the final analysis was performed in nine patients (13 plaques) (four males and five females; age 64±6 years). In this group, all patients were receiving aspirin at the time of inclusion. Clinical data are also summarised in Table 1. Six patients (eight plaques) received atorvastatin 20 mg/day and the remaining three patients (five plaques) received a standard hypocholesterolaemic diet for 3 months. Their serum lipid profile [total cholesterol, low-density lipoprotein (LDL) and high-density lipoprotein (HDL) cholesterol] was evaluated before and after therapy.

The present study was approved by the local ethical committee. All subjects gave their written informed consent before entering the study.

Table 1. Clinical features of patients from groups A and B at time of enrolment

Patient (PN)	Age (yrs)	Sex	CHO (mg/dl)	TG (mg/dl)	Therapy	Diabetes	Smoker	Hypertension	TIA/stroke
Group A									
M.F. (1)	87	M	210	157	Ticlopidine, simvastatin	Yes	No	Yes	No
P.G. (2)	65	F	195	88	Aspirin	No	Yes	Yes	No
G.G. (3)	73	M	190	94	None	Yes	Yes	No	No
G.E. (4)	83	M	215	110	None	No	No	Yes	No
B.F. (5)	72	M	220	125	Aspirin	No	Yes	Yes	No
A.E. (6, 10)	72	F	205	155	Ticlopidine, simvastatin	No	No	Yes	No
S.V. (7)	86	F	198	96	Aspirin	Yes	No	Yes	Yes
B.V. (8)	76	M	215	156	Aspirin	Yes	No	Yes	Yes
C.M. (9)	71	M	190	141	Ticlopidine	No	No	Yes	Yes
B.C. (11)	54	F	235	174	None	Yes	No	Yes	No
C.G. (12)	70	M	188	122	None	Yes	Yes	Yes	No
D.P. (13)	76	M	198	135	Ticlopidine	No	Yes	No	No
G.L. (14, 15)	80	M	190	128	Aspirin	Yes	Yes	Yes	Yes
P.A. (16)	80	M	157	165	Aspirin	Yes	Yes	No	Yes
Group B									
M.I. (1)	66	M	223	90	Aspirin	No	No	No	No
M.R. (2)	62	F	223	85	Aspirin	No	No	Yes	No
P.M. (3)	55	F	318	74	Aspirin	No	No	No	No
G.E. (4, 5)	60	F	256	151	Aspirin	No	No	No	No
M.G. (6, 7)	56	F	259	162	Aspirin	No	No	No	No
D.E. (8)	73	F	290	155	Aspirin	Yes	No	No	No
F.L. (9, 10)	65	M	244	152	Aspirin	No	No	No	No
C.L. (11)	74	M	143	96	Aspirin	Yes	No	No	No
B.B. (12, 13)	64	F	243	118	Aspirin	No	No	No	No

PN plaque number, *CHO* total cholesterol, *TG* triglycerides, *TIA* transient ischaemic attack

Ultrasound studies

An ultrasound study was performed in all patients at the time of enrollment in order to identify plaque structure and size and to position a skin marker at the level of the carotid bifurcation. The carotid arteries were examined by B-mode ultrasound, combining high-resolution imaging and Doppler spectral analysis, with the use of a high-frequency imaging probe (7.5–9 MHz) and a Siemens Sonoline Omnia System (Siemens Medical Solutions USA, Inc., Malvern, PA, USA).

In group A patients, plaques were classified by means of their echostructure, according to standardised published methodology [26]:

Class I
=uniformly anechogenic
Class II
=predominantly hypoechogenic with >50% hypoechogenic area
Class III
=predominantly echogenic with >50% echogenic area
Class IV
=uniformly echogenic
Class V
=unclassified plaques

The luminal surface was also characterised as follows:

1 =regular
2 =irregular, with recess between 0.4 and 2 mm in depth and width
3 =irregular with recess of more than 2 mm in depth and width
4 =unclassified

For group B, only patients showing plaques with an echostructure of class II–IV and a luminal surface of class 3 were recruited.

^{99m}Tc-IL2 scintigraphy

Radiolabelling of IL2 was performed using a two-step technique as previously described [27]. Briefly, the N_3S bifunctional chelating agent *S*-tetrahydropyranylmercaptoacetyl (thio-2,3,5,6 tetrafluorophenyl)-adypoilglycylglycine was first complexed with ^{99m}Tc at 80°C for 20 min at pH 1.8 and then conjugated to the protein at pH 9.5, at room temperature, for 45 min. After labelling, ^{99m}Tc-IL2 was purified from ^{99m}Tc-pertechnetate and from other non-IL-2 impurities by reverse phase chromatography using 0.1 g tC2 columns (Sep-Pak, Waters, Milford, MA, USA) eluted with acidified ethanol. The radiochemical purity of the protein was tested by instant thin-layer paper chromatography and trifluoroacetic acid precipitation [27].

^{99m}Tc-IL2 scintigraphy was performed in all patients of group A, 3–5 days before surgical endoarterectomy. In group B, ^{99m}Tc-IL2 scintigraphy was performed both before and after 3 months of treatment with atorvastatin or hypocholesterolaemic diet. Planar and tomographic (single-photon emission computed tomography; SPECT) images of the neck were acquired 60 min after intravenous injection of 111–185 MBq of ^{99m}Tc-IL2. The acquisition time had previously been optimised in preliminary studies [24, 25]. On the basis of ultrasound scanning, a skin marker was drawn over the plaque for better localisation. The clinician who performed the analysis of scintigraphic images was unaware of the patient's clinical data. SPECT image analysis was performed by tridimensional reconstruction and correction for deep attenuation, using a Hanning filter and an attenuation coefficient of 0.125 cm^{-1}. Eight to ten transaxial sections, each 2 cm thick, were reconstructed from the origin of the common carotid upwards. ^{99m}Tc-IL2 uptake was calculated at the level of the carotid bifurcation, behind the submandibular salivary gland: a circular region of interest (ROI) was drawn over this area (also identifiable by a skin marker previously positioned using ultrasound) and a similar ROI was drawn over the spinal bone marrow as background. In order to quantify the degree of ^{99m}Tc-IL2 uptake, a carotid plaque to background radioactivity ratio (T/B) was calculated after normalising ROI counts per ROI size.

Endoarterectomy and carotid artery preparation

Endoarterectomy was performed in all patients from group A, 5–7 days after the ^{99m}Tc-IL2 scan. Surgery was performed under general anaesthesia using conventional carotid endoarterectomy involving longitudinal arteriotomy, plaque extraction and closure of the arteriotomy without a patch. Patient nos. 6 and 14 were recruited twice at an interval of 3–6 months because they were re-operated on the contralateral artery. After surgery, carotid plaque was put in saline and immediately processed as recently described by Bonanno et al. [28]. Briefly, carotid specimens were opened longitudinally and examined in order to assess the presence of thrombi and atherosclerotic plaques. From each sample, seven sections of 2-μm thickness were cut, one at the beginning, five in the middle and one at the end of the lesion; all sections were fixed in formalin and paraffin embedded for morphological studies such as cell population determination and measurement of intimal thickness. The remainder of the carotid sample, including the inner media and the atherosclerotic plaque, was extensively washed in phosphate-buffered saline (PBS) to remove blood cells adherent to the surface of the plaque, minced into fine pieces and digested overnight at 37°C with type I collagenase (Sigma Chemical Co., St. Louis, Mo, USA) at 900 units/ml in RPMI 1640 tissue culture medium supplemented with 10% foetal calf serum. The resulting cell suspension containing all cells initially present in atherosclerotic plaque and intima was filtered through a 150 mesh nylon net, washed in PBS and stained for flow cytometry. Cell death associated with the incubation procedure was negligible (cell viability 95% by trypan blue exclusion test), and the incubation procedure did not affect the cell antigenic properties or cause detectable cell activation, as previously described. After collagenase digestion, the inner media remaining undigested was removed, thus avoiding contamination from smooth muscle cells from the arterial wall.

Flow cytometry analysis of digested plaques

Flow cytometry was performed as described elsewhere [28]. Briefly, the following antigens were tested: CD3 for T lymphocytes, CD19 for B lymphocytes, factor VIII for endothelial cells, CD68 for monocytes/macrophages, α-smooth muscle actin-1 (SMA) for smooth muscle cells and CD25 for IL2R-positive cells. Since in the first five plaques, monoclonal antibodies to CD19 and factor VIII did not demonstrate any significant labelling, only monoclonal antibodies to CD3, CD68, SMA and CD25 were used for all other patients. Therefore, each suspension was divided into five aliquots containing at least 10×10^4 cells each in order to assess: (1) unstained cells (negative control); (2) non-specifically stained cells [a mixture of phycoerythrin (PE) and fluorescein isothiocyanate (FITC) secondary conjugated antibodies]; (3) CD3/SMA (double labelling: CD3 PE-labelled and SMA FITC-labelled monoclonal antibodies); (4) CD68 (FITC-labelled monoclonal antibodies); (5) CD25 (FITC-labelled monoclonal antibodies). Anti-human CD3, anti-human CD68 and anti-human CD19 were used at a dilution of 1:100 (Dako, Glostrup, Denmark); anti-α-SMA and anti-factor VIII at a

dilution of 1:100 (Sigma, St.Louis, MO, USA); and anti-human CD25 at a dilution of 1:50 (Neomarker/Lab Vision CA, USA). Peripheral blood mononuclear cells isolated by Ficoll-Paque (Pharmacia, Uppsala, Sweden) gradient centrifugation from peripheral blood of healthy donors were used as positive controls for lymphocytes and monocytes, and smooth muscle cells isolated by elastase digestion from human carotid media were used as positive controls for smooth muscle cells.

After three washes in PBS, all cell suspensions were analysed with a flow cytometer (Coulter Epics XL; Coulter Corporation, Hialeah, FL, USA) equipped with an air-cooled, 15-mW argon ion laser operating at 488 nm. The forward scatter, the side scatter and the fluorescent intensity and compensation were set using both positive and negative controls. Data were analysed using the Listmode Analysis of the Epics CL software. The amount of each cell population was calculated counting the positive events after subtraction from the non-specific events falling in the region of the positive control. The whole cell population was obtained by summing positive events for CD3, CD68 and α-SMA subpopulations. Single subsets were also quantified as percent values.

A quality control panel was developed both for testing the quality of the specimens and for setting the side and forward scatters, the intensity of fluorescence and the colour compensation. The quality control panel included: peripheral blood mononuclear cells, cultured human smooth muscle cells from tunica media and cell plaque samples stained with an irrelevant antibody or with secondary conjugated antibodies omitting the primary antibody.

Immunohistochemistry for conventional and confocal microscopy

To characterise the cell populations of plaques, single-label immunohistochemistry was also performed on four of the five sections obtained from the centre of the plaque. Sections were deparaffinised and endogenous peroxidase activity was blocked with H_2O_2. Primary antibodies (anti-human CD3, dilution 1:100, Dako, Glostrup, Denmark; anti-human CD68, dilution 1:100, Dako, Glostrup, Denmark; anti-α-SMA, dilution 1:100, Sigma, St.Louis, MO, USA; anti-human CD25, dilution 1:50 Neomarker/Lab Vision CA, USA) were applied for 1 h at room temperature followed by a secondary antibody incubation (biotinylated goat anti-mouse, dilution 1:40, or goat anti-rabbit, dilution 1:20) for 30 min at room temperature. Then, avidin-biotin amplification (ABC kit, Dako, Glostrup, Denmark) was applied for 30 min at room temperature. Incubation with 0.1% 3′,3′-diaminobenzidine (Dako, Glostrup, Denmark) and H_2O_2 at room temperature for 5–10 min produced a brown reaction pigment. Light haematoxylin counterstaining was used to visualise all nuclei in the tissue sections. One section was incubated with a mixture of irrelevant monoclonal reagents with a similar isotype, as negative control.

The number of positive cells for each antibody was counted at a magnification of ×40 in the plaque shoulder region and in the cap itself using a grid with an area of 0.22 mm^2. A mean of ten randomly selected fields were counted for each section.

Statistical analysis

Calculated T/B ratios (from analysis of SPECT images) were correlated with histological results (obtained on both sections and flow cytometry) using regression analysis (group A). Ultrasound scores were correlated with the scintigraphic score and with histological findings by Spearman's rank test (group A).

Differences between T/B ratios and between LDL cholesterol before and after treatment were analysed by Wilcoxon test (group B).

Results

Transversal study

On visual inspection of planar images, clearly defined ^{99m}Tc-IL2 uptake was observed in eight plaques (seven patients). Analysis of SPECT sections allowed definite plaque visualisation in 14 out of 16 plaques (Fig. 1). Table 2 reports the individual T/B ratios calculated on SPECT sections as well as the ultrasound features of patients participating in the transversal study. The T/B ratios ranged from 1.6 to 3.47 with a mean of 2.50±0.52. It is noteworthy that no significant correlations were observed between T/B ratios and the plaque echostructure or

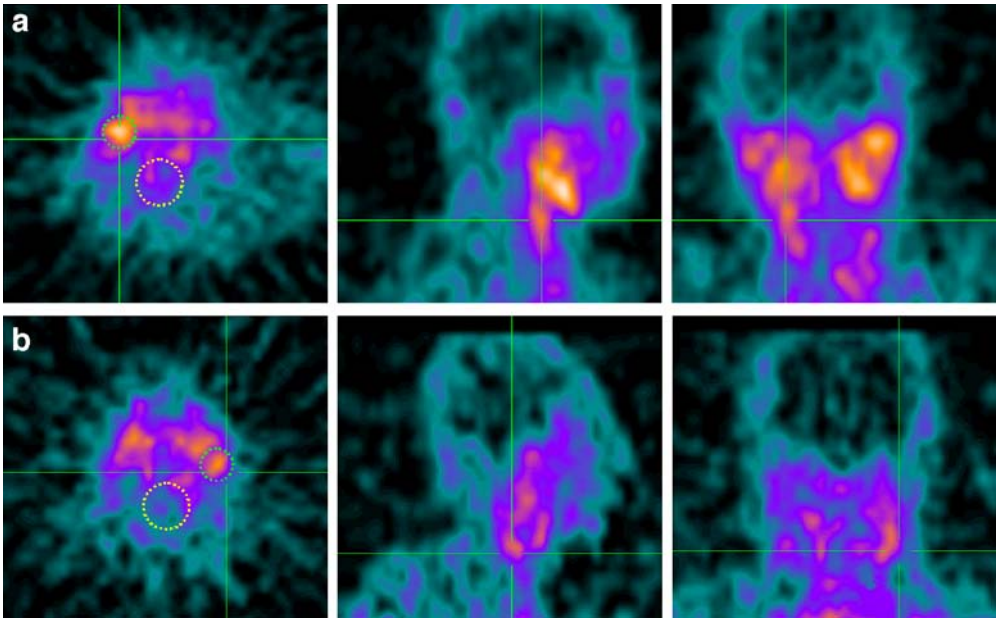

Fig. 1. ^{99m}Tc-IL2 scintigraphy in two patients with a plaque in the right (**a**) and the left (**b**) carotid. Images are transaxial, sagittal and coronal views at the level of the carotid bifurcation. Calculated T/B ratios were 3.47 and 2.63, respectively. After surgery, these plaques showed 40% (**a**) and 20% (**b**) of CD25+ cells at cytometry. Images also show the ROIs used for calculation of the T/B ratio in transaxial sections (*yellow circle*, target; *green circle*, background)

Table 2. Cyto-histological, scintigraphic and ultrasound parameters of plaques from group A patients

Plaque	FACS			Immunohistochemistry		US score		^{99m} Tc-IL2
	Cells (no.)	CD25+ (%)	CD25+ (no.)	CD25+ (%)	CD25-positive cells	Class	Type	T/B ratio
1	200,000	20.0	40,000	30	All plaque and tunica media cells	3	2	2.63
2	250,000	5.0	12,500	10	SMC	2	2	2.58
3[a]	–	–	–	25	SMC, endothelial cells	3	2	3.13
4	100,000	9.0	9,000	10	SMC	ND	ND	2.35
5	350,000	40.0	140,000	60	All plaque and tunica media cells	1	2	3.47
6	200,000	6.3	12,600	5	Foam cells	2	2	2.30
7	50,000	0.5	250	0	No inflammatory cells	2	1	1.89
8	50,000	0.5	250	0	No inflammatory cells	2	2	2.20
9	50,000	1.5	750	5	Lymphocytes, endothelial cells	2	2	1.94
10	70,000	2.3	1,610	5	Lymphocytes, endothelial cells	3	2	2.00
11[a]	–	–	–	0	No inflammatory cells	3	2	1.60
12[a]	–	–	–	25	Lymphocytes, foam cells, SMC	3	3	2.39
13	100,000	5.0	5,000	5	Lymphocytes	2	3	2.61
14	180,000	10.0	18,000	10	Lymphocytes, SMC	4	3	3.12
15	140,000	7.5	10,500	10	Lymphocytes, SMC	4	3	2.84
16	190,000	12.0	22,800	15	Lymphocytes, macrophages	1	1	3.00

Plaques no. 6 and 10 both relate to patient A.E. and plaques no. 14 and 15 both relate to patient G.L. (cf. Table 1)
ND not done, *SMC* smooth muscle cells, *CD25+* IL2 receptor-positive cells, *FACS* fluorescent activated cell sorter
[a] Flow cytometric analysis of these plaques was not performed due to technical problems related to the low number of cells available

the luminal surface as assessed by ultrasound (Spearman rank test).

The results of flow cytometric and morphometric studies are also summarised in Table 2. CD25+ cells were found at cytometric analysis in all plaques studied, although with a wide range of variability (from 0.5% to 40% of total plaque cells). Moreover, we observed that CD25 was expressed not only on the surface of T lymphocytes and macrophages, but also in other cell populations, particularly on smooth muscle cells (Fig. 2). A significant correlation was observed between T/B ratios (calculated on SPECT images) and the following three cyto-morphometric parameters: the percentage of IL2R-positive cells on histology (r=0.707; p=0.002), the percentage of IL2R-

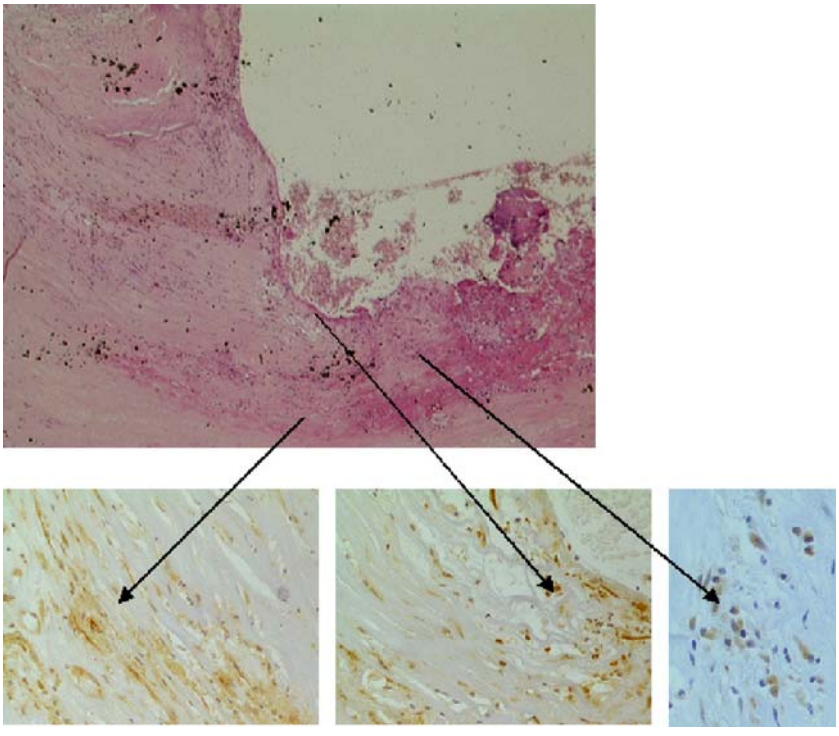

Fig. 2. Histological analysis of a carotid plaque showing 25% of CD25+ cells. *Upper image*: haematoxylin/eosin staining. *Lower images*: immunoperoxidase staining with a monoclonal antibody anti-CD25. CD25 positivity was detected on lymphocytes (*lower right image*) and on smooth muscle cells (*lower left and central images*)

positive cells on flow cytometry (r=0.711; p=0.006) and the absolute number of IL2R-positive cells on flow cytometry (r=0.774; p=0.002) (Fig. 3). No significant correlation was observed between plaque echostructure or luminal surface type as assessed by ultrasound and the percentage of CD25-positive cells (Spearman rank test). The mean ^{99m}Tc-IL2 uptake on carotid plaques and the percentage of IL2R-positive cells at histology were both significantly higher in smokers (2.89± 0.36 vs 2.11±0.32, p=0.002, and 20.0±17.7% vs 6.9± 9.9%, p=0.025, respectively).

Longitudinal study

On visual inspection of planar images, clearly defined ^{99m}Tc-IL2 uptake was observed in five plaques (three patients). Analysis of SPECT sections allowed definite plaque visualisation in nine out of 13 plaques. In patients belonging to group B, T/B ratios at entry were comparable to those observed in group A, ranging from 1.49 to 3.02 with a mean of 2.23±0.46. This suggested that there were no significant differences between the groups in terms of the amount of IL2R-positive cells in carotid plaques.

As expected, treatment with atorvastatin resulted in a significant 38% reduction in the LDL cholesterol level (97.17±17.17 mg/dl vs 179.00±35.45 mg/dl; p=0.028) (Fig. 4c). In contrast, in patients who received dietary recommendations, no changes were observed in the LDL cholesterol level (158.67±44.09 mg/dl vs 146.00±55.75 mg/dl; p=NS).

The mean ^{99m}Tc-IL2 uptake in plaques decreased significantly in patients treated with atorvastatin (1.75± 0.50 vs 2.16±0.44; p=0.012), while it was unchanged in those on a hypocholesterolaemic diet (2.33±0.45 vs 2.34± 0.5). In particular, while a reduction in the T/B ratio was observed in eight out of eight plaques of patients after therapy with atorvastatin, in patients treated with diet the uptake was increased in two, decreased in two and unchanged in one (Fig. 4a,b).

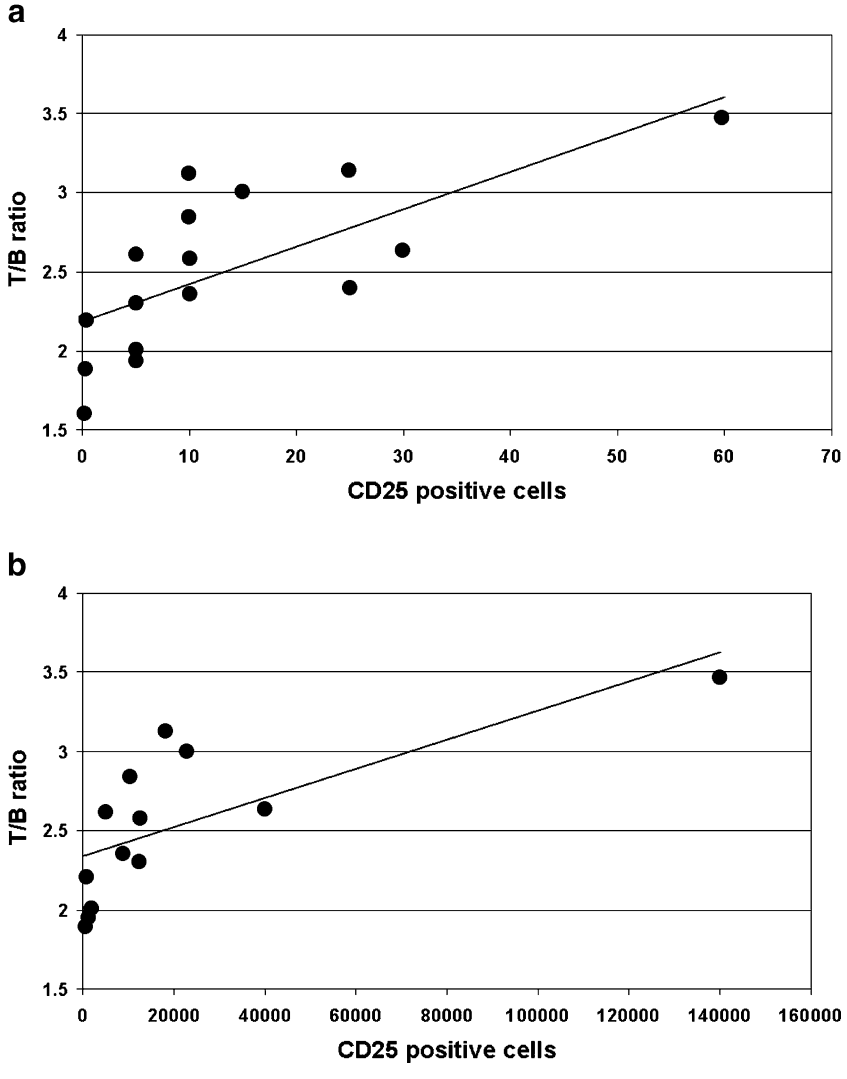

Fig. 3. Correlation of T/B ratios on SPECT sections with the percentage of IL2R-positive (CD25+) cells at histology (**a**) and with the absolute number of CD25+ cells obtained after plaque digestion and flow cytometry (**b**)

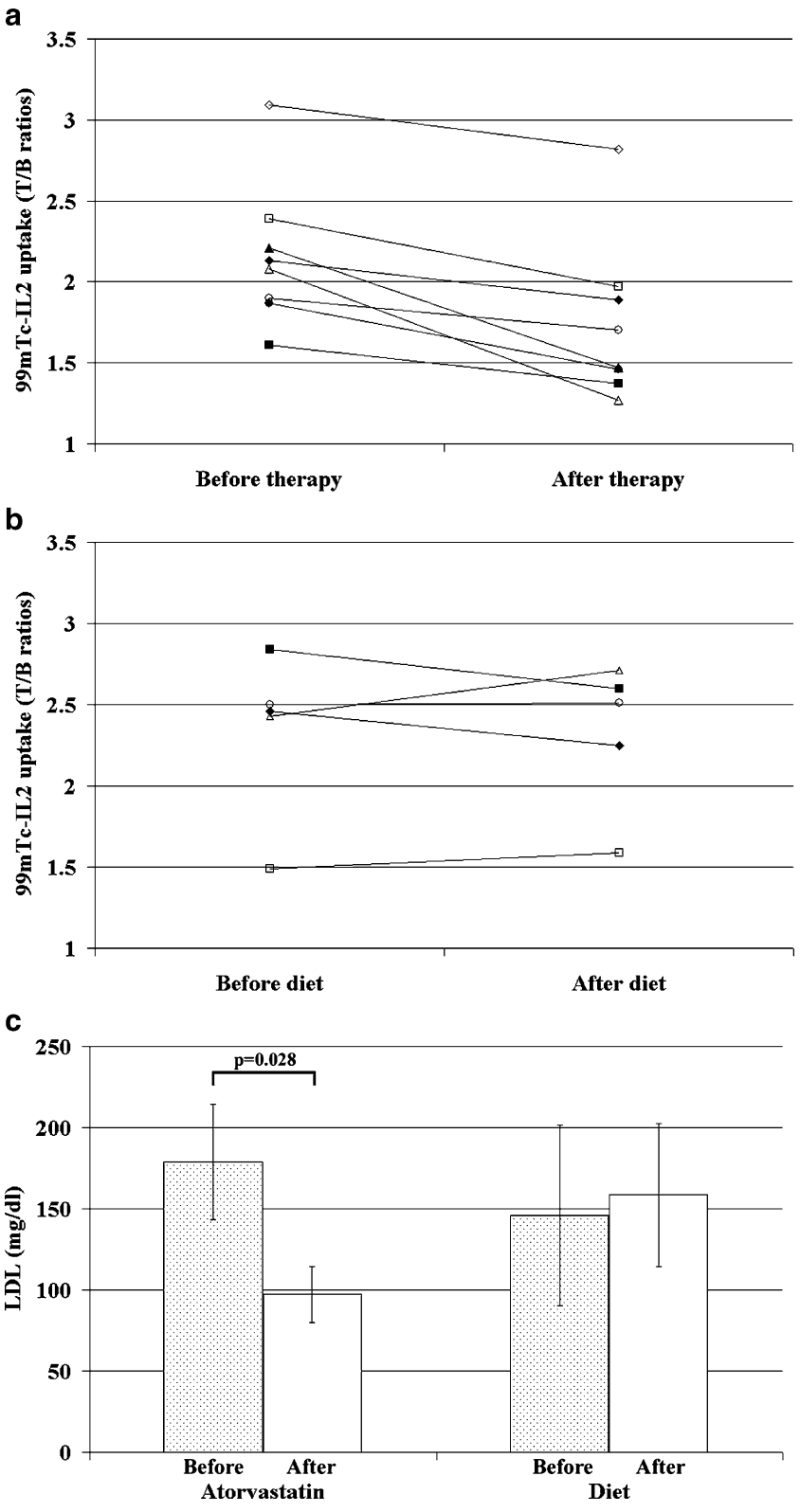

Fig. 4. a,b ^{99m}Tc-IL2 uptake in carotid plaques before and after atorvastatin (**a**) or hypocholesterolaemic diet (**b**). **c** Serum LDL values before and after atorvastatin treatment or hypocholesterolaemic diet

Discussion

The major finding of the present study was that the amount of ^{99m}Tc-IL2 taken up by carotid plaques correlated strongly with both the percentage and the absolute number of IL2R-positive cells isolated by cytofluorimetry in the plaque, indicating that this imaging modality can allow non-invasive in vivo quantification of plaque inflammation. Many data indicate that structural changes following inflammatory damage within the plaque are critical in

promoting plaque rupture [2, 3], and our results suggest that ^{99m}Tc-IL2 scintigraphy is a useful tool to identify "vulnerable" plaques which are more prone to cause clinical events. Another important finding is the observation that, in our patient cohort, the mean ^{99m}Tc-IL2 uptake in carotid plaques was significantly higher in smokers than in non-smokers, while it was not associated with other stroke risk factors like hypertension, hypercholesterolaemia and diabetes. A similar association with smoking status was also observed with the percentage of IL2R-positive cells found at histology and, although not statistically significant, with the percentage and absolute number of IL2R-positive cells found at flow cytometry. These findings support an influence of cigarette smoking on plaque inflammation, as also reported by others [29].

Considering that a certain degree of ^{99m}Tc-IL2 uptake could be measured in the majority of plaques studied, it would be important to define a T/B cut-off value of clinical significance. This could be particularly useful in symptomatic patients bearing carotid stenoses (angiographically evaluated) of less than 70% or in asymptomatic patients with stenoses greater than 70%, both situations in which endoarterectomy intervention is not considered mandatory [30, 31].

Despite the high correlation between the uptake of ^{99m}Tc-IL2 and the number of IL2R-positive cells described above, the results of cytofluorimetry studies revealed that within plaques, IL2Rs are expressed not only on inflammatory cells (lymphocytes and monocytes) but also on smooth muscle cells, the major population of cells obtained after plaque digestion. This finding has already been reported in atopic asthmatic serum-sensitised smooth muscle cells [32]. In this respect, it has also been postulated that direct cell–cell and cytokine-mediated interactions between activated leucocytes and injured vascular cells could lead to the proliferation of smooth muscle cells [33]. Several reports have also suggested that smooth muscle cells within the plaque show a "synthetic" phenotype, being able to produce cytokines and growth factors, including transforming growth factor-β, basic fibroblast growth factor (β-FGF) and vascular endothelial growth factor (VEGF), and to respond to platelet-derived growth factor (PDGF) or to other possible growth stimulators [1].

Another interesting observation of our study is that the ultrasound characteristics of plaques did not show any correlation with the amount of detectable expression of CD25 (as evaluated by histology) or the scintigraphic results. Thus, some patients classified as being at high risk of plaque rupture by ultrasound showed low CD25 expression and vice versa. This finding deserves further investigation before a conclusion is drawn, but it may not necessarily be a discrepancy and could be explained by the existence of different types of vulnerable plaque [34]. This evidence rather suggests that the concomitant use of radiological techniques, such as ultrasound and MRI, that are able to detect "morphological" aspects of vulnerable plaques (sub-occlusive thrombi, intra-plaque haemorrhage etc.) and nuclear medicine techniques that address "physiopathological" aspects of plaque vulnerability (lymphocyte/macrophage infiltration, smooth muscle cell amount etc.) may be advisable to increase the specificity of detection of vulnerable plaques.

Several other approaches have been proposed for the imaging of vulnerable plaques: the use of radiolabelled LDLs, and of oxidised LDLs in particular, has been considered optimal to obtain histopathological information of the plaque, considering that they specifically bind to the scavenger receptor expressed by macrophages [10]. In fact, labelled LDLs, or oxidised LDLs, accumulate in infiltrated but not in fibrocalcific plaques, which are considered at lower risk for acute ischaemic events [12]. Thus, oxidised LDL scintigraphy may be useful for the detection of plaque instability. However, purification and labelling of autologous LDLs can be performed only in a few specialised centres. Moreover, labelled LDLs do not provide any information on the presence of infiltrating T lymphocytes that are the pathogenetic cause of macrophage activation and plaque vulnerability [2, 3, 6]. ^{99m}Tc-annexin-V has been proposed for the visualisation of apoptotic macrophages on atherosclerotic lesions in the hypercholesterolaemic rabbit. The degree of ^{99m}Tc-annexin-V uptake has been found to correlate directly with the lesion severity and macrophage content [19]. Nevertheless, it is not clear whether apoptotic macrophage content can be representative of vulnerability.

Other investigators have reported imaging of vulnerable plaques using ^{18}F-FDG PET in both humans [14–17] and animal models [13, 18]. Although ^{18}F-FDG seems a very promising and easily available radiopharmaceutical for imaging atheromas, it must be considered that it is a non-specific agent. Indeed, its uptake in large plaques correlates with the presence of both macrophages and smooth muscle cells but also with patient age and cholesterol levels. Thus, ^{18}F-FDG tends to reflect the metabolic status of the plaque whereas ^{99m}Tc-IL2 shows the presence of activated lymphocytes/monocytes/macrophages and smooth muscle cells expressing the CD25 receptor, and is thus a true marker of plaque instability. The use of PET and PET/CT scanners significantly improves plaque detection, and it is to be welcomed that in future ^{18}F-labelled IL2 will be available.

Finally, we demonstrated that the uptake of ^{99m}Tc-IL2, expressed as the T/B radioactivity ratio, decreases significantly after treatment with atorvastatin. Although the study population comprised a small number of patients, our data support previous findings demonstrating a favourable effect of statins on plaque stabilisation [35] and in particular the supposition that statins may directly modulate inflammation within the plaque.

In summary, our results show that ^{99m}Tc-IL2 scintigraphy is able to detect the presence of inflammation in carotid plaques and allows monitoring of changes in such inflammation during treatment. Possible limitations to the use of ^{99m}Tc-IL2 scintigraphy for carotid plaque visualisation are, on the one hand, the complexity of IL2 labelling and purification and, on the other hand, the lack of anatomical detail and the low resolution of gamma camera imaging for small objects. In view of these limitations, IL2 labelling

with ^{18}F is under development. The use of PET/CT or SPECT/CT technology could allow better plaque detection and localisation.

Acknowledgements. This study was partially supported by the Italian Ministry of Public Education, by the International Atomic Energy Agency (IAEA) and by GE-Amersham Healthcare. This paper was awarded with the 2004 Marie Curie award by the European Association of Nuclear Medicine (EANM).

References

1. Ross R. Atherosclerosis—an inflammatory disease. N Engl J Med 1999;340:115–26
2. Schumacher H, Kaiser E, Schnabel PA, Sykora J, Eckstein HH, Allenberg JR. Immunophenotypic characterisation of carotid plaque: increased amount of inflammatory cells as an independent predictor for ischaemic symptoms. Eur J Vasc Endovasc Surg 2001;1:494–501
3. Spagnoli LG, Mauriello A, Sangiorgi G, Fratoni S, Bonanno E, Schwartz RS, et al. Extracranial thrombotically active carotid plaque as a risk factor for ischemic stroke. JAMA 2004; 92:1845–52
4. Muller JE, Stone PH, Turi ZG, Rutherford JD, Czeisler CA, Parker C, et al. Circadian variation in the frequency of onset of acute myocardial infarction. N Engl J Med 1985;13:1315–22
5. Carr SC, Farb A, Pearce WH, Virmani R, Yao JS. Activated inflammatory cells are associated with plaque rupture in carotid artery stenosis. Surgery 1997;122:757–63
6. Spagnoli LG, Bonanno E, Mauriello A, Palmieri G, Partenzi A, Sangiorgi G, et al. Multicentric inflammation in epicardial coronary arteries of patients dying of acute myocardial infarction. J Am Coll Cardiol 2002;40:1579–88
7. Schönbeck U, Mach F, Sukhova GK, Murphy C, Bonnefoy JY, Fabunmi RP, et al. Regulation of matrix metalloproteinase expression in human vascular smooth muscle cells by T lymphocytes: a role for CD40 signaling in plaque rupture? Circ Res 1997;81:448–54
8. Yuan C, Tsuruda JS, Beach KN, Hayes CE, Ferguson MS, Alpers CE, et al. Techniques for high resolution MR imaging of atherosclerotic plaque. J Magn Reson Imaging 1994;4:43–9
9. Virgolini I, Rauscha F, Lupattelli G, Angelberger P, Ventura A, O'Grady J, et al. Autologous low-density lipoprotein labelling allows characterization of human atherosclerotic lesions in vivo as to presence of foam cells and endothelial coverage. Eur J Nucl Med 1991;18:948–51
10. Iuliano L, Signore A, Vallabhajosula S, Colavita AR, Camastra C, Ronga G, et al. Preparation and biodistribution of 99m technetium-labelled oxidized LDL in man. Atherosclerosis 1996;126:131–41
11. Leitha T, Staudenherz A, Gmeiner B, Hermann M, Huttinger M, Dudczak R. Technetium-99m labelled LDL as a tracer for quantitative LDL scintigraphy. II. In vivo validation, LDL receptor-dependent and unspecific hepatic uptake and scintigraphic results. Eur J Nucl Med 1993;20:674–9
12. Iuliano L, Signore A, Violi F. Uptake of oxidized LDL by human atherosclerotic plaque. Circulation 1997;96:2093–4
13. Ogawa M, Ishino S, Mukai T, Asano D, Teramoto N, Watabe H, et al. ^{18}F-FDG accumulation in atherosclerotic plaques: immunohistochemical and PET imaging study. J Nucl Med 2004;45:1245–50
14. Hanif MZ, Ghesani M, Shah AA, Kasai T. F-18 fluorodeoxyglucose uptake in atherosclerotic plaque in the mediastinum mimicking malignancy: another potential for error. Clin Nucl Med 2004;29:93–5
15. Tatsumi M, Cohade C, Nakamoto Y, Wahl RL. Fluorodeoxyglucose uptake in the aortic wall at PET/CT: possible finding for active atherosclerosis. Radiology 2003;229:831–7
16. Rudd JH, Warburton EA, Fryer TD, Jones HA, Clark JC, Antoun N, et al. Imaging atherosclerotic plaque inflammation with [^{18}F]-fluorodeoxyglucose positron emission tomography (symptomatic, unstable plaques accumulate more ^{18}FDG than asymptomatic lesions). Circulation 2002;105:2708–11
17. Yun M, Jang S, Cucchiara A, Newberg AB, Alavi A. ^{18}F FDG uptake in the large arteries: a correlation study with the atherogenic risk factors (cc age/chol and FDG). Semin Nucl Med 2002;32:70–6
18. Lederman RJ, Raylman RR, Fisher SJ, Kison PV, San H, Nabel EG, et al. Detection of atherosclerosis using a novel positron-sensitive probe and 18-fluorodeoxyglucose (FDG) (cc SMC/Mac and FDG). Nucl Med Commun 2001;22:747–53
19. Kolodgie FD, Petrov A, Virmani R, Narula N, Verjans JW, Weber DK, et al. Targeting of apoptotic macrophages and experimental atheroma with radiolabeled annexin V: a technique with potential for noninvasive imaging of vulnerable plaque. Circulation 2003;108:3134–9
20. Prat L, Torres G, Carrió I, Roca M, Riambau V, Berna L, et al. Polyclonal ^{111}In-IgG, ^{125}I-LDL and ^{125}I-endothelin-1 accumulation in experimental arterial wall injury. Eur J Nucl Med 1993;20:1141–5
21. Qin G, Zhang Y, Cao W, An R, Gao Z, Li G, et al. Molecular imaging of atherosclerotic plaques with technetium-99m-labelled antisense oligonucleotides. Eur J Nucl Med Mol Imaging 2005;32:6–14
22. Knight LC. Non-oncologic applications of radiolabeled peptides in nuclear medicine. Q J Nucl Med 2003;47:279–91
23. Robb RJ, Greene WC, Rusk CM. Low and high affinity cellular receptors for interleukin 2. Implications for the level of Tac antigen. J Exp Med 1984;160:1126–46
24. Signore A, Chianelli M, Annovazzi A, Rossi M, Maiuri L, Greco M, et al. Imaging of active lymphocytic infiltration in coeliac disease with ^{123}I-Interleukin-2 and its response to diet. Eur J Nucl Med 2000;27:18–24
25. Annovazzi A, Biancone L, Caviglia R, Chianelli M, Capriotti G, Mather SJ, et al. ^{99m}Tc-Interleukin-2 and ^{99m}Tc-HMPAO granulocyte scintigraphy in patients with inactive Crohn's disease. Eur J Nucl Med Mol Imaging 2003;30:374–82
26. Consensus sur la morphologie et le risque des plaques carotidiennes. A paraître dans Cerebro Vascular Disease. Basel: Karger;1997:N° 3
27. Chianelli M, Signore A, Fritzberg A, Mather SJ. ^{99m}Tc-interleukin-2: the development of technetium-99m labelled Interleukin 2: a new radiopharmaceutical for in vivo detection of mononuclear cell infiltrates in immune mediate diseases. Nucl Med Biol 1997;24:579–86
28. Bonanno E, Mauriello A, Partenzi A, Anemona L, Spagnoli LG. Flow cytometry analysis of atherosclerotic plaque cells from human carotids: a validation study. Cytometry 2000; 39:158–65
29. Chou ET, Minutello RM, Parikh M, Bergman G, Chiu Wong S, Hong MK. Can we identify vulnerable patients at risk for ST-segment elevation myocardial infarction based on their clinical characteristics? Coron Artery Dis 2004;15:467–69
30. North American Symptomatic Carotid Endarterectomy Trial Collaborators. Beneficial effect of carotid endarterectomy in symptomatic patients with high-grade carotid stenosis. N Engl J Med 1991;325:445–53
31. European Carotid Surgery Trialists' Collaborative Group. Endarterectomy for moderate symptomatic carotid stenosis: interim results from the MRC European Carotid Surgery Trial. Lancet 1996;347:1591–3

32. Hakonarson H, Kim C, Whelan R, Campbell D, Grunstein MM. Bi-directional activation between human airway smooth muscle cells and T lymphocytes: role in induction of altered airway responsiveness. J Immunol 2001;166:293–303
33. Miller DD, Karim MA, Edwards WD, Schwartz RS. Relationship of vascular thrombosis and inflammatory leukocyte infiltration to neointimal growth following porcine coronary artery stent placement. Atherosclerosis 1996;124:145–55
34. Naghavi M, Libby P, Falk E, Casscells SW, Litovsky S, Rumberger J, et al. From vulnerable plaque to vulnerable patient: a call for new definitions and risk assessment strategies: part I. Circulation 2003;108:1664–72
35. Sukhova GK, Williams JK, Libby P. Statins reduce inflammation in atheroma of nonhuman primates independent of effects on serum cholesterol. Arterioscler Thromb Vasc Biol 2002; 22:1452–8